LA-UR- 10-05174

Approved for public release; distribution is unlimited.

Title:	Progress on detection of liquid explosives using Ultra-Low Field MRI
Author(s):	Michelle Espy, Shermiyah Baguisa, David Dunkerley, Per Magnelind, Andrei Matlashov, Tuba Owens, Henrik Sandin, Larry Schultz, Algis Urbaitis, Petr Volegov
Intended for:	Applied Superconductivity Conference 2010, Washington DC, August 1 - 6, 2010

Los Alamos
NATIONAL LABORATORY
EST. 1943

Los Alamos National Laboratory, an affirmative action/equal opportunity employer, is operated by the Los Alamos National Security, LLC for the National Nuclear Security Administration of the U.S. Department of Energy under contract DE-AC52-06NA25396. By acceptance of this article, the publisher recognizes that the U.S. Government retains a nonexclusive, royalty-free license to publish or reproduce the published form of this contribution, or to allow others to do so, for U.S. Government purposes. Los Alamos National Laboratory requests that the publisher identify this article as work performed under the auspices of the U.S. Department of Energy. Los Alamos National Laboratory strongly supports academic freedom and a researcher's right to publish; as an institution, however, the Laboratory does not endorse the viewpoint of a publication or guarantee its technical correctness.

Form 836 (7/06)

Progress on detection of liquid explosives using Ultra-Low Field MRI

Michelle Espy, Shermiyah Baguisa, David Dunkerley, Per Magnelind, Andrei Matlashov, Tuba Owens, Henrik Sandin, Larry Schultz, Algis Urbaitis, Petr Volegov

Abstract— **Nuclear magnetic resonance (NMR) and magnetic resonance imaging (MRI) methods are widely used in medicine, chemistry and industry. Over the past several years there has been increasing interest in performing NMR and MRI in the ultra-low field (ULF) regime, with measurement field strengths of 10 – 100 microTesla and pre-polarization fields of 30 – 50 mTesla. The real-time signal-to-noise ratio for such measurements is about 100. Our group at LANL has built and demonstrated the performance of SQUID-based ULF NMR/MRI instrumentation for classification of materials and detection of liquid explosives via their relaxation properties measured at ULF, using T_1, T_2, and T_1 frequency dispersion. We are also beginning to investigate the performance of induction coils as sensors. Here we present recent progress on the applications of ULF MR to the detection of liquid explosives, in imaging and relaxometry.**

Index Terms— **Ultra low field MRI, ultra-low field NMR, relaxometry.**

I. INTRODUCTION

NUCLEAR magnetic resonance (NMR) and magnetic resonance imaging (MRI) are traditionally performed in magnetic fields greater than 1 Tesla, because the magnetization and thus signal strength scale with the applied magnetic field. However, despite the reduced signal strength, NMR and MRI at much lower fields have always been of interest [old refs]. Recently, numerous applications of ULF NMR and MRI have been demonstrated with SQUID sensors. Some examples include J-coupling spectroscopy [Clarke], enhanced T_1 contrast for cancer detection [Clarke], imaging compatible with biomagnetic measurements such as magnetoencephalography [us, germans?], and applications where low-field instrumentation provides unique advantages [refs?]. One such instance is classification of liquids at a security check-point [], where the power of NMR/MRI assessing chemical properties is desired, but limiting exposure to high magnetic fields and imaging through metal or foil-lined containers is desired. In airport security checkpoints, there is a strong desire to determine the chemical content of materials being carried on board aircraft quickly and non-invasively. Since 2006, there has been increased concern about the threat of liquid explosives being carried on to aircraft, which has prompted costly and onerous travel restrictions on the volume of liquids passengers are allowed to carry on board. The restrictions are motivated by the fact that presently deployed screening methods are not capable of providing such screening of chemical composition. ULF MR methods may provide a path forward,

The obvious draw-back of low signal at ULF has been partially overcome by the use of pre-polarizing methods [], and SQUID detectors are used to enhance sensitivity. At ULF, NMR chemical shift spectroscopy is not possible. Instead, NMR relaxometry, a more indirect method, is required for the liquid identification application. The Department of Homeland Security lists ~ 100 items including liquids (oxidizers, fuels, and mixtures) to exclude from airplanes. Preliminary results indicate relaxometry using T_1 and T_2 alone has some ability distinguish threat liquids from benign items [refs]. However, relaxation parameters physical properties connected to chemical composition of a liquid, but not a direct measurement of the chemical composition. It is likely that additional parameters (such as frequency dispersion, diffusion) will be required for robust identification [].

In this paper we present several new results from our group's development of a ULF MRI relaxometer. These include (1) development of a dual polarization coil configuration to image thicker samples (field-of-view is ~ 25cm radius and ~20 cm depth), (2) investigation of frequency dispersion in T_1 as an additional classification parameter, (3) and the implementation of induction coils to improve sensitivity.

II. AIRPORT SCREENING OF LIQUIDS

Presently there are numerous screening technologies deployed and being tested at airport security check-points. However, most of these are looking for hidden weapons (x-ray and millimeter wave) or the presence of material residue from making bombs (mass spectrometry) and most of these methods focus on solids. Recently very sophisticated x-ray machines, such as [SUST14], have been deployed that are able to distinguish liquids from solids. There is evidence that this approach might also be able to identify at least some threat liquids, although accurate determination of a variety of threat liquids remains speculative. X-ray methods rely not on detection of chemical signature but on density and atomic number. As with the MR relaxation measurements we propose, this is more indirect. Moreover, the approach may

Manuscript received 3 August 2010. This work was supported in part by the U.S. Department of Homeland Security.

All authors were with Los Alamos National Laboratory, MS- D454 Los Alamos, NM 87545 USA. 505-412-8705; fax: 505-665-4507; e-mail: espy@lanl.gov).

S. Baguisa is also with Ryerson University

D. Dunkerley is also with Clarion College

have difficulties achieving sufficiently low alarm rates in case of complicated bottle shapes. Mass spectrometry, which does give chemical structure, presently relies on either opening bottles up in the case of liquids, or swiping surfaces.
Raman scattering, in which the frequencies and intensities of Raman-scattered photons reflect the conformation and electronic states of the probed molecule, can also provide a chemical signature. Electromagnetic methods based on multi-

frequency microwave evanescent field sensors [SUST15] measure the conductivity and dielectric relaxation of liquids, to provide a chemical fingerprint in a very short amount of time (~ 1 s). These approaches are all limited to single bottles, which remains too slow for rapid screening, and are used for random checks. Moreover, liquids in metal and metalized containers cannot be inspected by these techniques. Thus far, none of these approaches has been widely deployed or demonstrated for liquids.

An important benefit of the MR approach is the ability to probe chemical structure. Indeed, MR spectroscopy is an ideal technology for screening liquids. However, conventional instrumentation, employing magnetic fields > 1 T, may present an unacceptably large risk to the public, due to the exposure to magnetic fields sufficiently strong to attract metal objects. Operationally such a system would likely be unable to image items inside conductive packaging such as drinks in foil or cans. At the time of this writing, owing to lack of another screening technology, airport rules require that all of a passenger's carry-on liquids be restricted to 100 ml (~ 3-ounce bottles) and that all of the bottles be placed in a single one-quart, zip-lock bag. This is known as the "3-1-1" rule.

III. Results

A. *MagViz: ULF MRI Relaxometers*

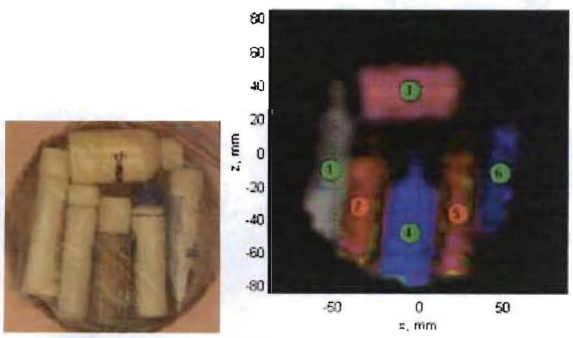

Fig. 1. Images and results from MagViz "2A" for 3-1-1 bag screening. (Left) Photograph of a sample "3-1-1" bag. (Right) Pseudo-color relaxation weighted MRI of the bag at left. Relaxation parameters are compared against a database as described in [SUST].

Previously we have described efforts to build a 7-channel ULF MRI relaxometer system constructed to non-invasively inspect liquids at a security check-point for the presence of hazardous material. The instrument, known as MagViz "2A" was deployed to the Albuquerque International Airport in December, 2008. Results from that instrument are shown in Figure 1. Imaging and classification methods are described fully in [SUST]. Relaxation weighted images are constructed and computed relaxation parameters of the detected objects are compared against database entries.

The "2A" system was designed to demonstrate the proof-of-concept for ULF MRI relaxometry as a screening tool. The system had a field of view over a radius of ~ 25 cm and a depth of ~ 10 cm, to accommodate the average "3-1-1" bag configuration.

While there is much work that remains to validate the relaxometry approach, and to expand the material data-base, the Department of Homeland Security, wished us to proceed with the design of a second system that would accommodate larger samples (screening tubs, small carry-on bags). To this end, we designed a unit capable of screening over a field of view of radius ~ 25 cm and a depth of ~ 20 cm.

A schematic of the MagViz "2B" system is shown in Figure 2. A representative pulse sequence is shown in Figure 3.

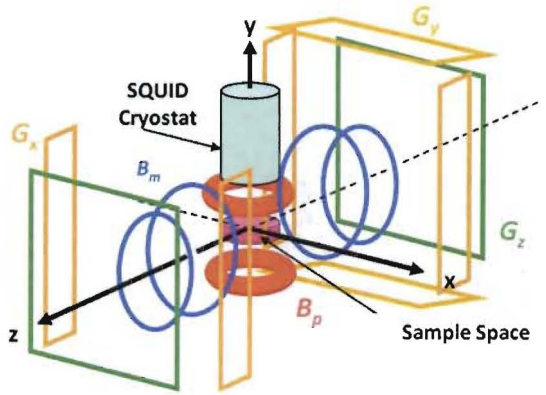

Fig. 2. Schematic of coil set for MagViz "2B".

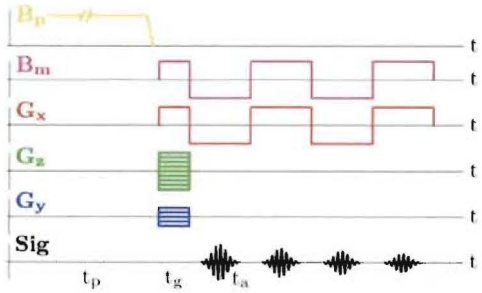

Fig. 3. Pulse sequence.

This system was largely similar to the "2A" design however the scheme for pre-polarization included a dual-coil design as shown in Figure 2. One coil is wrapped around the cryostat and the other located below the sample. The pre-polarization coils are capable of being operated in series with a current of ~ 65 Amperes. At this current we measured a field of 75 mT at the coil surfaces and ~ 50 mT in the center of the sample volume. The coils are resistive, but cooled with liquid nitrogen. Total resistance for the coil set is ~ 1 Ω.

Both MagViz systems use seven 2nd order wire-wound gradiometer pick-up coils, which are 90 mm in diameter; the baseline (coil separation along the gradiometer axis) is also 90 mm. The noise of the system at the gradiometers (magnetic field noise spectral density at 1 kHz, referred to the pick-up coil) is 1.5-2 fT/√Hz.

After some pre-polarization time (ranging from 1-3 seconds) the B_p field is turned off non-adiabatically (i.e. fast enough that the magnetization remains in the original direction, $dB_p/dt \geq \gamma B_m^2$) with a ramp-down time of 7

milliseconds. The much weaker measurement field, B_m, is applied perpendicular to B_p to start precession. The intensity of B_m typically ranges from 50 μT to 100 μT (proton Larmor frequencies from ~2 kHz to 4 kHz). A measurement field echo technique is used to reduce the effects of magnetic field inhomogeneities. Such a sequence would be impossible with a conventional MRI system where the measurement field is generated by large permanent or superconducting magnets with fixed field orientations. Gradient field echoes in the *x*-direction are also used. The encoding scheme is based on the 3D Fourier protocol with a frequency encoding gradient $G_x = dB_z/dx$ and two phase encoding gradients, $G_z = dB_z/dz$ and $G_y = dB_z/dy$ [SUST2], [SUST28]. The voxel size produced is 5 mm x 30 mm x 10 mm in the x, y, and z directions, respectively.

From the sequence described above relaxation weighted images are constructed. The measurement of T_2 is performed at the lower field value B_m. However, T_1 is determined by repeating the pulse sequence for two differing polarization times, ~ 1 and 3s, and using the difference in the measured signal amplitude between the two polarizing. Thus we are actually measuring the value of T_1 in the higher (~50 mT) prepolarization field.

Computed relaxation parameters of the detected objects are compared against database entries. The method is capable of classification of multiple samples in random configurations, to depths up to ~ 200 mm. Figure 4 shows a 2D image acquired inside a soft-sided suitcase with dimensions ~ 56 x 36 x 20cm deep. In the center of the suitcase, which was packed with clothing and toiletries, two ~0.5 l bottles were placed, one with water and the other with 40% stabilized hydrogen peroxide, which is used as a threat surrogate. However, we were still able to make a successful determination of T1 and T2 values. The time to acquire the images shown was ~ 80 s. The pulse sequence could be shortened to ~ 60 s, however we ran with long delay time between imaging steps (~ 2s) as a precaution. We were also able to identify an aluminum soda can in the suitcase (data not shown). The ability to see through non-ferrous metals and foils is unique to the ULF regime. For example the skin depth for aluminum at 4 kHz is 1.3 mm whereas at 42 MHz (the precession frequency of protons in a ~ 1T field) the depth is ~ 13 microns. We, and others, have shown the ability to image through aluminum cans [SUT31],[SUST32]. Eddy currents are present after field pulsing, and persist for tens of milliseconds. This limits our ability to look at materials with relaxation times less than 50 ms inside such packaging. As the materials we investigate are liquids, relaxation times are typically hundreds of milliseconds to a few seconds and this does not affect our data. However, the presence of magnetic material, such as zippers, in luggage is likely, and will shorten relaxation times. Thus further research is required. Although we successfully showed the depth sensitivity required for carry-on bag screening, and some immunity to magnetic material, there remain many advances required for baggage screening by ULF MRI. This work does point to progress at screening large bins of segregated liquids, which also may be of more immediate benefit to relaxing carry-on liquid restrictions.

B. Depth Sensitivity and Induction Coils

The data shown in Figure 5a demonstrates the sensitivity of the system for depth. The phantom is 5 water bottles with ~ 30 ml stacked in a diagonal pattern. In these images, only the lower coil was operated. Thus the magnetic field at the top of the sample was only ~ 17 mT. Never-the-less it is clear the SQUIDs are quite sensitive to the upper samples. The middle samples are in a field of ~ 40 mT and at a distance of ~ 10cm. The lower phantom is at ~ 15 cm and is barely visible owing to the large distance from the sensors.

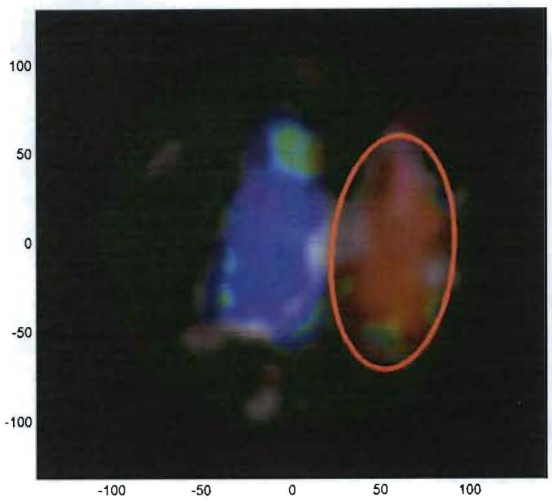

Fig. 4. Image of threat in suitcase

For security screening applications it is likely that use of cryogenically cooled sensors, such as SQUIDs, will be undesirable. Therefore we have also begun investigating the possibility of room temperature sensors in the form of untuned induction coils. These coils are described in detail elsewhere [Ref Andrei's paper]. Briefly, there are 7-coils arranged with one coil at center and six coils surrounding. Each coil has 90 mm outer diameter, 20 mm inner diameter and 14 mm height. It consists of 1400 turns of AWG24 copper wire. L = 70 mH, R = 20 Ohm. The field transfer coefficient is about 70 V/mT at 3.3 kHz.

Figure 5b shows the same phantom with the addition of these coils to the bottom, just above the lower pre-polarization coil set. The coils have a sensitivity of 20-25 fT/√Hz at 3.3 kHz, which is ~ a factor of 5 higher than the SQUIDs in our instrument. However, the increase in resolution for the lower two coils of the phantom are a factor of 4 -5. While the coils are lower in sensitivity than the SQUIDs, it is clear that they help offset the reduced signal due the greater distance. We are presently investigating whether the use of such coils, placed both above and below the imaging volume, would provide sufficient SNR to replace the SQUIDs entirely.

C. Frequency Dispersion

The Department of Homeland Security lists ~ 100 items including liquids (oxidizers, fuels, and mixtures) to exclude from airplanes. Preliminary results indicate MagViz can distinguish several using T_1 and T_2 alone. These represent physical parameters connected to chemical composition of a liquid, but not a direct measurement. It is likely additional

parameters (such as frequency dispersion) will be required for robust identification. Using a field-cycling relaxometer (Stelar SmartTracer) we are studying how the frequency dependence of T_1 can be used as an added classification parameter. One advantage of ULF MRI is the ability to easily change field strengths. These data are shown in Fig. 6.

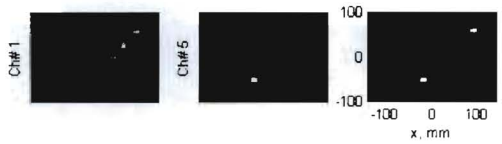

Figure 5

IV. Future Directions

Presently our work for DHS is focusing on increasing the data-base of both threats and streams of commerce, adding frequency dispersion, and determining false-positive and false-negative rates by calculating receiver operator curves. We are also in the process of building an NMR relaxometer for secondary bottle screening.

We continue to investigate ULF MRI instrumentation and applications to anatomical imaging as well.

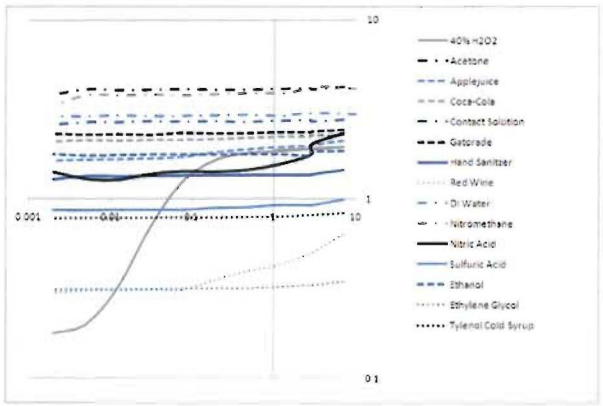

Figure 6.

It is clear that ULF MRI is possible. To be practical, it must enable unique applications and provide unique information. Screening through metal, instrumentation compatible with MEG, and possibly more informative T_1 contrast are limited examples. Spatial resolution thus far lags well behind traditional MRI.

ULF MRI has strong potential application because of compatibility with neuromagnetic measurements such as MEG/EEG (see also Magnelind 2EC-01), unique tissue contrast at ULF, and potential for low-cost and portable anatomical imaging systems (such as battlefield MRI machines). We are also working, under separate funding, on such applications. There remains enormous room for advancement.

Acknowledgment

This project was funded in part by the Science and Technology Directorate, U.S. Department of Homeland Security.

References

[1] McDermott R, Lee S-K, ten Haken B, Trabesinger A, Pines A, and Clarke J 2004 Microtesla MRI with a superconducting quantum interference device, *Proc. Natl. Acad. Sci. USA* **101** 7857-7861.

[2] Zotev V S, Matashov A N, Volegov P, Urbaitis A V, Espy M A, and Kraus R H Jr., 2007 SQUID-based instrumentation for ultralow-field MRI, *Supercond. Sci. Technol.* **20**, S367-S373.

[3] Packard M, and Varian R, 1954 Free nuclear induction in the earth's magnetic field, *Phys. Rev.*, **A93,** 941.

[4] Macovski A, and Conolly S, 1993 Novel approaches to low-cost MRI, *Mag. Res. Med.* **30**, 221-230.

[5] McDermott R, Lee S, ten Haken B et al., 2002 Liquid-state NMR and scalar couplings in microtesla magnetic fields, *Science* 295 2247-2249.

[6] Zotev V, Matlashov A N, Volegov P, et al., 2007 Multi-Channel SQUID System for MEG and Ultra-Low Field MRI, *IEEE Trans Supercond.*, **17**(2), 839-842.

[7] Lee S K, Mössle M, Myers W, et al., 2005 SQUID-detected MRI at 132 μT with T_1-weighted contrast established at 10 μT-300 *mT, Magn. Res. Med.* **53**, 9-14 .

[8] Koenig S H, Brown R D, 1990 Field-cycling relaxometry of protein solutions and tissue: implications for MRI, *Progr. NMR Spectrosc.* **22**, 487-567.

[9] Zotev V S, .Matlashov A N , Volegov P et al., 2008 Microtesla MRI combined with MEG", *J. Mag. Res.* **194** (1) , 115-120.

[10] Zotev V S , Matlashov A N, Volegov P L, et al., April 2008 IEEE/CSC & ESAS EUROPEAN SUPERCONDUCTIVITY NEWS FORUM, No. 4,, http://www.ewh.ieee.org/tc/csc/europe/newsforum/pdf/ST31_brainFinal_020708.pdf

[11] Kraus R, Volegov P, Matlachov A, Espy M, 2008 Toward Direct Neural Current Imaging by Resonant Mechanisms at Ultra-Low Field, *Neuroimage* **39**, 310- 317.

[12] Volegov P, Matlashov A, Kraus R H, 2006 Ultra-low field NMR measurements of liquids and gases with short relaxation times, *J. Mag. Res.* **183**, 134–141.

[13] Magnelind P, Matlashov A, Volegov P, Espy M, 2009 Ultra-low Field NMR of UF_6 for ^{235}U Detection and Characterization, *IEEE Trans. Appl., Supercond*19(3)1 816-818

[14] *Smith's HI-SCAN 6040aTiX,* 64 Clarendon Road, Watford, Herts WD17 1DA, UK

[15] *EMISENS EMILI* Karl-Heinz-Beckurts Str. 13, D-52428 Jülich, GmbH, info@emisens.de

[16] Fan N Q, Clarke J, 1991 Low-frequency nuclear magnetic resonance and nuclear quadrupole resonance spectrometer based on a DC superconducting quantum interference device" *Rev. Sci. Instrum.* **62** 1453–9.

[17] Yesinowski J P, Buess M L, Garroway A N, 1992 Detection of N-14 and Cl-35 in cocaine base and hydrochloride using NQR, NMR and SQUID techniques, *Anal. Chem.* **67** 2256–63.

[18] Tonthat D M, Clarke J, 1996 Direct current superconducting quantum interference device spectrometer for pulsed nuclear magnetic resonance and nuclear quadrupole resonance at frequencies up to 5 MHz, *Rev. Sci. Instrum.* **67** 2890–3.

[19] He D F,Tachiki M, Itozaki H, 2008 N-14 NQR using a high-Tc rf SQUID with a normal metal transformer, *Supercond. Sci. Technol.* **21,** 015023 (4pp).

[20] Garroway A N, Buess M L, Miller J B et al., 2001 Remote Sensing by Nuclear Quadrupole Resonance", *IEEE Transactions on Geoscience and Remote Sensing*, **39** (6).

[21] Espy M,Flynn M, Gomez J et al., 2009 Applications of Ultra-low Field Magnetic Resonance for Imaging and Materials Studies", *IEEE Trans. Appl. Supercond.*, 19(3)1 835-838.

[22] Haacke E M, Brown R W, Thompson M R, Venkatesan R., 1999 Magnetic resonance imaging: physical principles and sequence design *Wiley-Liss New York.*

[23] Kimmic R, Anoardo E, 2004 Field-cycling NMR relaxometry *Prog. Nucl. Mag. Res. Spect.*, **44**, 257-320 .

[24] Bene G J, 1980 Nuclear magnetism of liquid systems in the Earth field-range, *Phys. Rep.* **58** (4), 213–267.

[25] Zotev V S, Matlashov A N, Volegov P et al. 2007 Multi-channel SQUID system for MEG and ultra-low-field MRI, *IEEE Trans. Appl. Supercond.* **17** 839-842.

[26] Supracon AG, http://www.supracon.com

[27] CRYOTON Co. Ltd., http://cryoton.webzone.ru

[28] Zotev V, Volegov P, Matlashov A et al., 2008 Parallel MRI at microtesla fields, *J. Magn. Reson.* **192,** 197-208.
[29] Pruessmann K P, Weigner M, Sheidegger M B et al., 1999 SENSE: Sensitivity Encoding for Fast MRI, *Magnetic Resonance in Medicine* **42**, 952-962.
[30] Georgescu B, Shimshoni B, Meer P, 2003 Mean Shift Based Clustering in High Dimensions: A Texture Classification example *Proc ninth Int'l Conf. Computer Vision.* 456-463.
[31] Matlachov A N, Volegov P L, Espy M A, George J S, Kraus R H 2004, SQUID-detected NMR in microtesla magnetic fields, *J. Magn. Reson.* 170 1–4.
[32] Mo¨ßle M, Han S-I, Myers W R, Lee S-K, Kelso N, Hatridge M, Pines A, Clarke J, 2006 SQUID-detected microtesla MRI in the presence of metal *J. Magn. Reson.* 179 146–151.
[33] Terranova by Magritek
[34] IMEDCO, http://www.imedco-shielding.com/englisch/intro.html